Razavian, R. S., Azad, N. L., & McPhee, J. (2013). A battery hardware-in-the-loop setup for concurrent design and evaluation of real-time optimal HEV power management controllers. International Journal of Electric and Hybrid Vehicles, 5(3), 177.

Final version published by Inderscience Publishers, and available at: https://doi.org/10.1504/IJEHV.2013.057604

A Battery Hardware-in-the-Loop Setup for Concurrent Design and Evaluation of Real-Time Optimal HEV Power Management Controllers

Reza Sharif Razavian

PhD Candidate,
Department of Systems Design Engineering
University of Waterloo
rsharifr@uwaterloo.ca

Nasser L. Azad

Assistant Professor
Department of Systems Design Engineering
University of Waterloo
nlashgarianazad@uwaterloo.ca

John McPhee

Professor
Department of Systems Design Engineering
University of Waterloo
mcphee@uwaterloo.ca

Abstract: We have developed a battery hardware-in-the-loop (HIL) setup, which can facilitate the process of design and evaluation of power management controllers for hybrid electric vehicles (HEVs) in a novel cost- and time-effective manner. Since the dynamics of the battery greatly affects the HEV power management controller design, and because such dynamic behavior is difficult to model, physical batteries and a real-time battery cycler are included in the setup for greater simulation fidelity. The setup employs a scaled-down battery HIL that reduces the development and testing efforts, while, by using Buckingham's Pi Theorem, maintains the required flexibility and enhances the control loop fidelity.

In this article, the application of the setup in integrating the development and the evaluation processes is shown. First, the setup is used for parameter identification of a simple control-oriented model of the battery, which is then used in the power management controller design. Finally, the real-time performance of the designed controller, programmed into an electronic control unit (ECU), is tested with the same setup in the realistic control environment. Furthermore, the battery HIL simulation results show that the designed controller is able to accurately capture the dynamics of the real system, by which the assumptions made in its design process can be confidently justified.

Copyright © 2009 Inderscience Enterprises Ltd.

Keywords: Cost-Effective Battery HIL, Hybrid Electric Vehicle, Optimal Power Management Controller, Battery Identification, Component Scaling, Model-Based Controller Design

Reference This paper should be referred to as follows: Razavian, R.S., Azad, N.L., McPhee, J. (xxxx) "A Battery Hardware-in-the-Loop Setup for Concurrent Design and Evaluation of Real-Time Optimal HEV Power Management Controllers", Int. J. Electric and Hybrid Vehicles, Vol. x, No. x, pp.xxxxxx.

Biographical notes: Reza Sharif Razavian received his BSc in Mechanical Engineering from Sharif University of Technology, Tehran, Iran, and his MASc in Systems Design from University of Waterloo, Waterloo, Canada. He is currently a PhD candidate in the Department of Systems Design Engineering at the University of Waterloo, and his area of research is in modeling of biomechanical systems.

Nasser Lashgarian Azad is an Assistant Professor in Systems Design Engineering at University of Waterloo. His primary research interests lie in modelling, estimation and control of complex dynamic mechanical and multi-domain physical systems, with special emphasis on advanced modelling and model reduction methods, sensitivity analysis techniques, nonlinear and optimal control, with applications to advanced vehicle systems, such as modern automotive powertrains and vehicle dynamics control systems.

John McPhee is a Professor in Systems Design Engineering at the University of Waterloo, Canada, and the NSERC/Toyota/Maplesoft Industrial Research Chair in Mathematics-based Modelling and Design. His main area of research is multibody system dynamics, with principal application to the analysis and design of vehicles, mechatronic devices, biomechanical systems, and sports equipment. He is a Fellow of the American Society of Mechanical Engineers and the Canadian Academy of Engineering. He was the Executive Director of the Waterloo Centre for Automotive Research until 2009, after which he spent a sabbatical year at the Toyota Technical Center in Ann Arbor, Michigan.

1 Introduction

HEVs have proven to be more fuel efficient than conventional vehicles. However, higher fuel economy cannot be achieved without an intelligent plan (the so called *supervisory* or *power management controller*) to decide on the power flow in the hybrid electric powertrain. Design and testing of such optimal power management controllers has been an interesting research topic in the past decade.

The major challenges in designing an optimal HEV power management controller are, first, the complexity of the system under control, and second, the uncertainty associated with the system input (i.e., the driver commands). The power management controller should command each component in such a way that the fuel consumption and/or emission is minimized while the driver command is followed, and the physical constraints of the system are not violated. In the early

stages of the development of HEVs, rule-based power management controllers were used; these plans, although being robust and simple to implement, do not result in optimal behavior and are difficult to tune.

Studies show that even a small reduction of 3% in HEV fuel consumption will save at least 6.5 million gallons of gas annually in the United States [1]. This has been the motivation for many researchers to invent model-based controllers in recent years, as these controllers have the potential to provide higher fuel economy compared to rule-based controllers [2].

One promising approach for the development of an optimal HEV power management strategy is Model Predictive Control (MPC) [3]-[5]. In MPC, the controller assigns the component set-points based on the dynamics and the inputs of the system. Thus, optimality of an MPC controller strongly depends on the accuracy of the model inside the controller. Similarly, Pontryagin's Minimum Principe (PMP) has shown strong potential in the development of optimal power management strategies [6]-[13]. In PMP, the integral minimization problem is reduced to local minimization of the Hamiltonian [14], which in turn, is reduced to tuning of the costates [10, 15]. Proper tuning of the costate requires a correct representation of powertrain components, especially the electrical storage system.

In recent studies [7, 8], we have developed real-time optimal controllers for a series HEV based on the solution of PMP for an off-line optimal control problem. The controllers have been shown to be mathematically optimal. However, the usefulness of these controllers, just as any other model-based controller, depends on the models upon which they are designed. On one hand, the control-oriented models must be as simple as possible to keep the computations manageable by the electronic control units (ECUs), and on the other hand, they should be able to represent the dynamics of the system accurately enough.

To evaluate the performance of such designed controllers, software simulations can be employed [8]. Although virtual modeling of the HEV powertrain components can provide valuable information about the system behavior, it may fail to depict all aspects of the control loop. Some aspects such as communication delays between different ECUs, real-time performance, and computational time for the power management controller cannot be easily simulated in the all-software environments. Moreover, the virtual models are only a representation of the real systems, and a certain level of error is unavoidable.

To study the real-time performance of the control loop, and to further enhance the fidelity of the simulations, physical components of the system can be included in the simulation in a Hardware-in-the-Loop (HIL) setup. In HIL simulations, usually the controller is programmed into a rapid-prototyping unit and the high-fidelity model of the system is solved in real-time. In addition, the critical components of the system can be realized as full-size or scaled physical components. In this work, because of the crucial impact of the electrical storage system in HEV power management controller design, physical batteries are included in the setup (sometimes called *component-in-the-loop* simulation).

The size of the components in HIL setups requires careful consideration. Unless the setup is designed for a specific target vehicle, the components have to be scaled properly to achieve the desired behavior in the target vehicle. One approach for component scaling is Buckingham's Pi Theorem in which the inputs, the outputs, or other parameters of the components are scaled in such a way that the dimensionless

groups of parameters in the target and scaled components are equal [16]. In the application of HIL for hybrid electric vehicles, Pi Theorem is shown to be an effective method for scaling the components to arbitrary sizes [17, 18]. In our scaled battery HIL, the same approach is taken to scale the battery cells to a full size battery pack.

In an HIL simulation, since some parts of the system are realized as virtual models and some other parts are physical systems, they have to work at the same time scale; otherwise, some dynamics and features of the system may not be captured correctly. Therefore, real-time simulation of the virtual model is essential in HIL simulations. For such applications, usually fixed-step solvers are more suitable, as the variable-step solvers do not provide a deterministic solution time. On the other hand, the fixed-step solvers show poor performance in stiff problems. Because of the absolute necessity for real-time operation, the fixed step solvers are preferred in HIL simulations. In this case, one approach to avoid stiff problems is to use the physical component instead of the stiff virtual model (e.g. using hydraulic circuits in [19, 20]).

In the area of simulation, HIL has been used extensively. In [19] and [21], the HIL setups were used for simulation and feasibility study of an electro-hydraulic system and a hybrid electric tram, respectively. An HIL setup was also used in [22] to increase the fidelity in simulation of a fuel cell vehicle. To find the efficiency maps and for model verification, an HIL setup (containing all the components of an HEV) was used in [23]. The campus-wide setup in [17], including several components in different labs across the campus, was used to simulate different component sizes in an HEV powertrian.

HIL simulation is a very handy tool in controller validation as well. For HEV controller simulation, HIL setups have been used in [17], [24]-[31]. HIL setup can also be used for lower-level controller development such as electric motor controller [32], ISG (integrated starter/generator) controller [33], semi-active suspension controller [34], and engine controller [35, 36]. For better EV controller design, road/tire interaction was realized in an HIL setup [37].

In this work a battery HIL setup is developed, which facilitates the design and evaluation of an HEV power management controller by integrating them into a novel unified structure, in which the controller design and the realistic real-time evaluation occur concurrently. The setup employs a rapid-prototyping electronic control unit (ECU) as the power management controller, a powerful real-time computer to solve the virtual vehicle model, and a real-time battery cycler for incorporating a physical battery into the simulations. The setup reduces the time and cost of development of HEV power management controllers, as it simultaneously gives the flexibility of software simulations that is essential in the controller design, and greater fidelity of the control loop that is required in the evaluation process. In the model-based controller design process, the setup is used to derive an accurate controller-oriented model. We also show how the parameters of the derived model and the battery cycler should be scaled using Buckingham's Pi Theorem to achieve accurate representations of the full size battery pack. Finally, real-time performance of the designed controller is evaluated with enhanced fidelity using the setup.

The rest of this article is organized as follows: Section 2 summarizes the basics of our optimal controller for a series HEV. In section 3, the details of the battery HIL setup are presented. Section 4 shows how the setup can be used to find the control-

Figure 1: Schematic of the series HEV

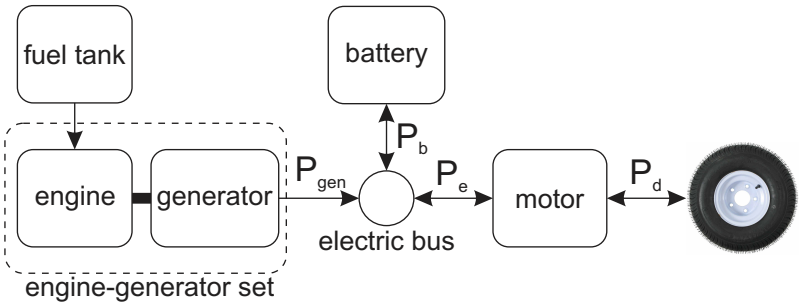

oriented model, and section 5 shows how the battery parameters can be scaled using Buckingham's Pi Theorem. Finally, section 6 presents the HIL simulation results and section 7 concludes the paper.

2 Real-Time Optimal Controller for a Series HEV

In a previous study [8], an optimal controller for a series HEV has been developed. Here a brief description of the controller is presented.

For the series HEV shown in Figure 1, a simple control-oriented model is assumed. In this control-oriented model, the battery is modeled according to (1) in which the battery parameters, V_{oc}, R and Q, are assumed to be independent of battery state of charge, SoC. This assumption will be justified in the later sections. (For a complete list of symbol descriptions please see the Nomenclature at the end of the paper).

$$\dot{SoC} = \frac{-V_{oc} + \sqrt{V_{oc}^2 - 4RP_b}}{2RQ} \tag{1}$$

The engine-generator set is also modeled in a simple manner according to:

$$\dot{m} = \alpha P_{gen} + \beta \tag{2}$$

with α and β being constants.

The electric motor is modeled as a power transducer, converting from electrical power to mechanical power and vice versa, with constant efficiency:

$$P_e = P_d \; \eta_m^{-sign(P_d)} \tag{3}$$

Finally, in the electric bus, the powers from the battery and the generator add together at 100% efficiency to form the total electric power:

$$P_{gen} + P_b = P_e \tag{4}$$

To form the optimal control problem, the cost function of (5) is considered. Pontryagin's Minimum Principle is then applied to this optimal control problem and it can be shown that the fuel-optimal solution is according to (6).

$$J = \int_0^{t_f} \dot{m}\, dt \tag{5}$$

$$P_b^* = \begin{cases} P_{max} & P_{max} < \bar{P} \\ \bar{P} & P_{min} < \bar{P} < P_{max} \\ P_{min} & \bar{P} < P_{min} \end{cases} \tag{6}$$

In the above control strategy, P_{min} and P_{max} are the time-varying maximum and minimum allowable battery power, and $\bar{P}$ is a constant value that should be tuned according to driving conditions to achieve charge sustenance. The value of $\bar{P}$ can be approximated with the method presented in [8].

Once the optimal battery power is determined, the power management controller calculates the optimal generator power according to (7), and this reference generator power is sent to the engine-generator set.

$$P_{gen}^* = P_e - P_b^* \tag{7}$$

The performance of the designed controller can be tested by applying it to a high-fidelity model of the series HEV powertrain [8, 38]; the schematic of the control loop in virtual simulations is shown in Figure 2a. The high-fidelity series HEV model in this *all-simulation* environment is developed in MapleSim, and consists of the engine-generator set, a multibody vehicle dynamics model, the electric motor, and the battery. The engine in this model is a mean-value engine model [39], and is torque-controlled by a sliding-mode controller [8]. The engine is coupled to a speed-controlled permanent-magnet DC generator. The torque and the speed set-points of the engine-generator set (T^* and ω^*) come from the optimal power management controller. Simultaneously, the 14-degree-of-freedom vehicle dynamics and traction motor models work together to drive the vehicle according to the reference velocity profile. The difference in the required power of the electric motor, P_e, and the generator output power, P_{gen}, is the amount of power that the battery should deliver or absorb. This battery power, P_b, is then fed to the chemistry-based Li-ion battery model [40], from which the battery SoC is calculated.

Since such a virtual simulation is done in one solver, the time scale of the controller and all parts of the model is the same; thus, real-time behavior of the controller cannot be evaluated properly. To study the real-time performance of the controller, communication issues, and computational limitations, an HIL simulation can be employed. Moreover, modeling error is unavoidable in simulations; thus, for a more accurate simulation, the battery model in the powertrain is replaced with physical battery cells, and a real-time battery cycler is used to drive the physical battery according to powertrain requirements (see Figure 2b). In the following section, the details of the HIL setup is presented.

Figure 2: (a) The control loop for the series HEV power management controller, in the all-simulation environment; (b) HIL simulation setup with ECU and physical battery

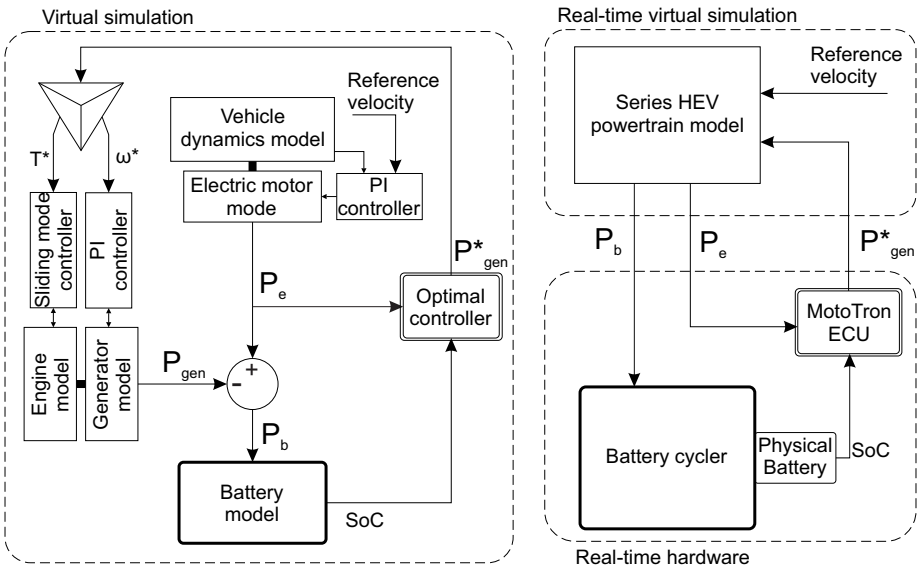

Figure 3: (a) The schematic of the battery HIL setup; (b) the setup developed

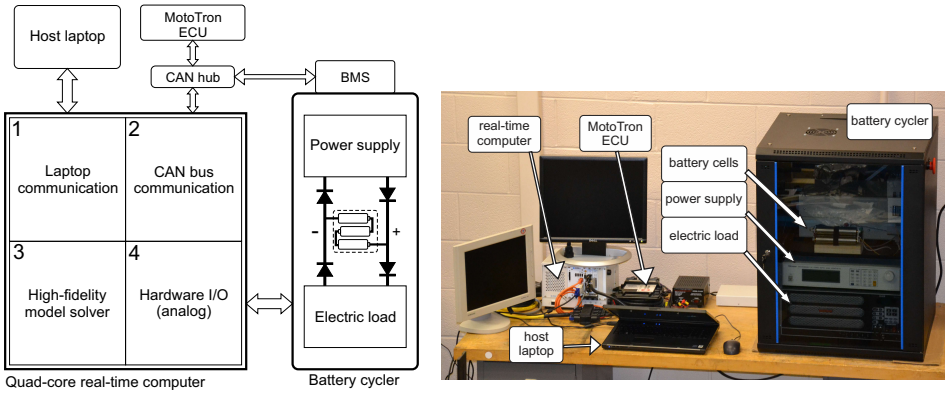

3 Hardware-in-the-Loop setup

The three core components in this HIL setup are: 1) an independent processing unit to run the controller procedure, 2) a powerful real-time computer to run the plant model, and 3) a real-time battery cycler to include physical battery cells in the simulations. Figure 3 shows the components in the HIL setup.

It is worthwhile to mention that the battery HIL setup developed is a scaled-down battery test bench – the battery under testing is not the same size as the battery pack in vehicles. Although in such a scaled simulation there is a small amount of error due to component scaling, the greater flexibility of the setup makes it ideal for development purposes. On the other hand, when the full-size battery pack is used, the results are only accurate for that particular battery pack, and simulating other battery sizes is not possible without the same scaling error. Therefore, working with a scaled-down battery test bench is not only more cost-effective, but it also provides the flexibility required for research and development purposes.

The real-time battery cycler consists of a power supply (Chroma 62024P) and an electric load (Ametek Sorensen SLH), which charge and discharge the battery cells (three GAIA 7.5Ahr Li-ion cells in series) in real-time, and according to powertrain simulation requirements.

For our HIL simulation, the designed controller is programmed into an Electronic Control Unit (ECU) from MotoTron. The automotive-based design of the ECU makes it an ideal choice for the HEV power management controller applications. The same high-fidelity powertrain model that had been previously used is solved deterministically by one core of a quad-core real-time computer (a National Instruments PXI computer) to provide the accurate sampling that the controller requires. The real-time computer is also responsible for controlling and facilitating the communications between different hardware, including the real-time battery cycler, the battery management system (BMS), the MotoTron ECU and the user interface (the host laptop), as shown in Figure 3a.

The communication channel between the ECU, the plant (virtual model in the real-time target), and the BMS is the Control Area Network (CAN). The real-time computer controls the battery cycler via a DAQ card and the battery cycler's analog interface.

As a result of the flexibility of the setup, the process of design and verification of the HEV power management controllers can be done in a very time- and cost-effective way. The calibratable build of the ECU enables real-time tuning of controller parameters. Moreover, high-fidelity powertrain models can be modified and re-deployed into the real-time computer very efficiently to accommodate, for example, different HEV architectures and component sizes (for an example, see [4]). Lastly, by employing the real-time battery cycler, real-time model solver, and realistic ECUs, it is possible to simulate the control loop with great accuracy, and without losing any real-time dynamics of the system, which is of great importance in rigorous evaluation of the HEV power management controllers.

In the following sections, the application of the HIL setup in effectively integrating the processes of design and evaluation of the HEV power management controller is presented.

4 Battery Identification

The development of HEV power management controllers is greatly affected by the properties of different components in the powertrain. The battery is one of the most

Table 1 Parameters in the identification problem

parameter	lower boundary	identified value	nominal value
R	1 mΩ	21 mΩ	19.5 mΩ
V_{oc}	10 V	10.699 V	10.80 V
Q	100 As	29729 As	27000 As

important components in a hybrid electric powertrain, and should be examined very closely before designing the power management controllers.

To design a better controller, an accurate control-oriented model that is tailored for a specific battery pack is essential. To identify the parameters that give the best representation of the cells, a parameter identification study has to be done on the battery.

As the developed battery HIL setup employs a scaled battery module, it can greatly reduce the time and cost of the development of HEV power management controllers. In this process, first, a simple control-oriented model for the few battery cells is found; then the model is scaled up to the target size. In this way, only a few battery cells is required for parameter identification, but the model can be scaled to any battery size, without a compromise in control-oriented model accuracy.

The controller-relevant parameter identification can be done off-line. In off-line identification methods, the system is excited, and the outputs are stored as a series of timed signals. The stored data is later compared with the output of the control-oriented model.

For the power management controller of section 2, the battery control-oriented model of which the parameters should be identified is given in (1). The parameters to be identified are $[V_{oc}, R, Q]$ with P_b and SoC being the input and the output, respectively.

In this study, the excitation power input is chosen as a pseudo-random binary sequence (PRBS), which contains a broad range of frequencies. The PRBS power input to the battery cells and the change in their state of charge are shown in Figure 4a.

Matlab's optimization toolbox is used to find the set of parameters that make the model in (1) give close results to the experimental data of Figure 4a. Among the optimization algorithms in Matlab, the Genetic Algorithm (GA) is one of the global optimization methods that can solve constrained optimization problems, and it is used in this parameter identification process. In this optimization problem, the objective function to be minimized is the sum of the square of error in each time step:

$$error = \sum \left(SoC_{model} - SoC_{experiment}\right)^2 \tag{8}$$

Since the parameters of the model in (1) have physical meaning, they cannot assume any number. For example, the open circuit voltage has to be close to the terminal voltage of the cells. Therefore, the lower limits presented in Table 1 are specified for the parameters in the optimization problem. Table 1 also presents the solution of the GA algorithm, with the initial population of $V_{oc} = 10.6V$, $R = 0.01\Omega$, $Q = 30000As$, population size of 100, and 100 generations.

Figure 4: The excitation input (P_b) and the resulting output of battery (SoC) used for (a) parameter identification, and (b) for model validation

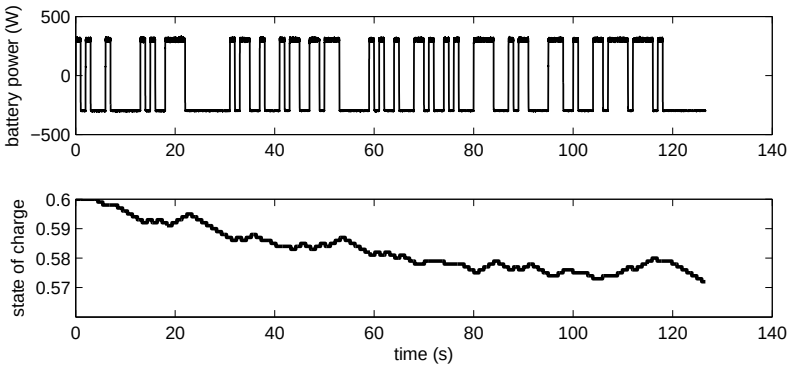

(a)

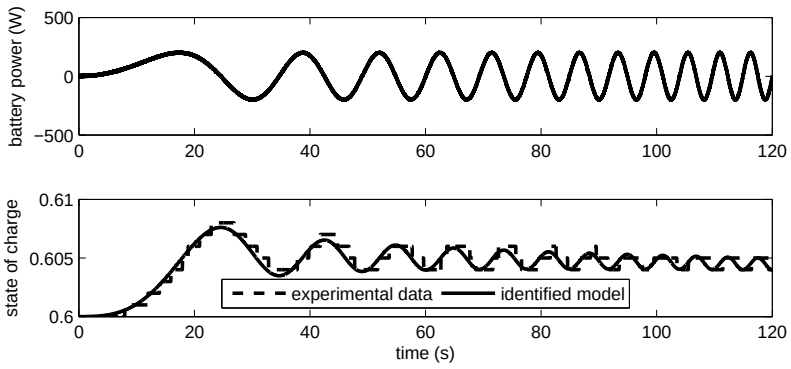

(b)

Table 2 Important parameters in battery analysis, their dimensions, and the corresponding dimensionless groups

parameter	dimension	related Pi group
P	$[M][L]^2[T]^{-3}$	primary
I	$[A]$	primary
τ	$[T]$	primary
V	$[M][L]^2[T]^{-3}[A]^{-1}$	$\pi_1 = P.V^{-1}.I^{-1}$
Q	$[A][T]$	$\pi_2 = I.t.Q^{-1}$
R	$[M][L]^2[T]^{-3}[A]^{-2}$	$\pi_3 = R.I^2.P^{-1}$

To validate the identified model, the batteries are excited with a different input (a chirp signal). The input power and the comparison of the state of charge between the identified battery model and the experimental data are shown in Figure 4b. It can be seen that the identified model can provide close behavior for different input frequencies. Thus the identified parameters can be used in the controller design process.

Once the control-oriented model for the three battery cells is found, it can be scaled to any target battery size. The process of scaling battery parameters is the subject of the next section.

5 Battery scaling in the HIL setup

Our battery HIL is a scaled-down setup. This means that the battery parameters, inputs, and outputs need to be scaled properly to get reasonable results. The battery scaling in this work has different aspects. First of all, the battery cells are simulating a full size battery pack; therefore, to get correct results, the input and output of the battery cycler (battery power and SoC, respectively) should be scaled appropriately. Moreover, for controller design, the identified control-oriented model of the battery cells should be scaled up to find the battery model of the target size.

Dimensional analysis is a well-established method, especially in fluid and thermal systems, to relate phenomena that are similar in behavior but different in parameters. In this study, Buckingham's Pi Theorem [16] is used to map parameters of batteries of different sizes. The approach chosen here is similar to that in [17].

The first two columns of Table 2 give the six parameters that need to be considered in battery analysis, as well as their dimensions in terms of four fundamental units: [M]: mass, [L]: length, [T]: time, and [A]: current.

The battery state of charge is another important parameter in battery analysis; however, it is a dimensionless parameter by itself, and we consider it as the output of the system. As long as other dimensionless groups of the systems are the same, the state of charge of the two systems will also prove equivalent. The battery power is the input to the battery cycler, and it is the parameter that must be scaled properly before being used to drive the battery. The final goal of this dimensional analysis is to identify such a scaling factor for the battery power.

Since the dimensional bundle of $[M][L]^2$ appears together, it can be considered as one fundamental unit, reducing the number of units to 3; therefore, the Pi Theorem states that the system (battery) can be presented by the $6 - 3 = 3$ dimensionless

groups [16]. There is no unique set of dimensionless groups, and in this analysis, τ, I, and P are chosen as the primary parameters. For the remaining parameters, dimensionless groups of π_1, π_2, and π_3 are formed and presented in the last column of Table 2.

5.1 Battery Scaling for HEV Simulation

In this experimental setup, three battery cells represent the full-size battery pack. As both systems have the same chemistry, the dynamics of the two systems are similar. The characteristic time, τ, is chosen to be the discharge time, which is related to the battery power and capacity. Since the battery pack and the cells in the HIL setup should behave similarly, the following relations have to be satisfied:

$$\pi_{1BP} = \pi_{1HIL} \tag{9}$$

$$\pi_{2BP} = \pi_{2HIL} \tag{10}$$

$$\pi_{3BP} = \pi_{3HIL} \tag{11}$$

In the above relations, the battery pack and the cells are denoted by the subscripts $_{\mathrm{BP}}$ and $_{\mathrm{HIL}}$, respectively. Substituting the Pi relations in Table 2 leads to:

$$\left[\frac{P}{VI}\right]_{BP} = \left[\frac{P}{VI}\right]_{HIL} \Rightarrow P_{HIL} = \frac{V_{HIL}}{V_{BP}}\frac{I_{HIL}}{I_{BP}}P_{BP} \tag{12}$$

$$\left[\frac{I\tau}{Q}\right]_{BP} = \left[\frac{I\tau}{Q}\right]_{HIL} \Rightarrow \frac{I_{HIL}}{I_{BP}} = \frac{Q_{HIL}}{Q_{BP}}\frac{\tau_{BP}}{\tau_{HIL}} \tag{13}$$

$$\left[\frac{RI^2}{P}\right]_{BP} = \left[\frac{RI^2}{P}\right]_{HIL} \Rightarrow \frac{P_{HIL}}{I^2_{HIL}} = \frac{P_{BP}}{I^2_{BP}}\frac{R_{HIL}}{R_{BP}} \tag{14}$$

By combining (12) and (13), one relation for power and capacity can be found:

$$P_{HIL} = \left[\frac{V_{HIL}}{V_{BP}}\frac{Q_{HIL}}{Q_{BP}}\frac{\tau_{BP}}{\tau_{HIL}}\right]P_{BP} \tag{15}$$

As the simulations have to be in real-time, the characteristic times of both systems are equal, and the scaling factor is reduced to:

$$\frac{P_{HIL}}{P_{BP}} = \frac{V_{HIL}}{V_{BP}}\frac{Q_{HIL}}{Q_{BP}} \tag{16}$$

Therefore, the battery power has to be scaled according to (16) before it is sent to the battery cycler to drive the battery cells.

It is important to notice that it may not be possible to map one system to the other by just a simple scaling. In this case, once the power is scaled according to (16), the last Pi relation, (14), may or may not be satisfied. This is because the internal resistance of the battery is an independent parameter and may not

Table 3 Nominal battery parameters used for scaling

parameter	RX400-h battery pack	GAIA cells
voltage (V)	288.0	10.8
capacity (Ahr)	6.5	7.5

be scalable. To better understand this situation, assume two battery cells with the same capacity and voltage, but different internal resistances. The difference may be due to build effects, battery wear, etc. As all of the parameters but the resistance are the same, the first two Pi groups, (12) and (13), are essentially the same for the two batteries, but nothing can be done to make (14) equal.

This apparent inconsistency with battery Pi groups can be solved by involving more parameters, such as an electro-chemical parameter; however, this type of analysis is out of the scope of this work, and the sole power scaling meets our requirements.

The Li-ion cells in the HIL setup are used to simulate HEV battery packs. The nominal values of the HIL battery parameters and the nominal values of a full-size battery pack (Lexus RX400-h) are presented in Table 3. With these parameters, the scaling factor can be calculated according to (17).

$$\frac{P_{HIL}}{P_{BP}} = \frac{V_{HIL}}{V_{BP}} \frac{Q_{HIL}}{Q_{BP}} = \frac{10.8\ V}{288.0\ V} \times \frac{7.5\ Ahr}{6.5\ Ahr} = 43.27 \times 10^{-3} \tag{17}$$

This means that the battery power calculated from the virtual HEV simulation has to be reduced by a factor of 43.27×10^{-3} before it is sent to the battery cycler. In this way, the output of the battery cycler (SoC) will be the same as a full-size battery pack.

5.2 Control-Oriented Model Scaling for Controller design

As was mentioned in the beginning of this section, for controller design purposes, the identified control-oriented model for the three battery cells should be scaled properly to a battery of target size.

The target battery in this study is the battery pack in a Lexus RX400-h vehicle with the nominal values specified in Table 3. The identified capacity and voltage of the battery cells can be scaled proportional to the nominal values, as in (18) and (19).

$$\frac{Q_{HIL}}{Q_{BP}} = \frac{Q_{ID}}{Q_{COM}} \Rightarrow Q_{COM} = Q_{ID} \times \frac{Q_{BP}}{Q_{HIL}} = 7.16\ Ahr \tag{18}$$

$$\frac{V_{HIL}}{V_{BP}} = \frac{V_{ID}}{V_{COM}} \Rightarrow V_{COM} = V_{ID} \times \frac{V_{BP}}{V_{HIL}} = 285.3\ V \tag{19}$$

In these relations, the nominal cell parameters in the battery HIL are denoted by the subscript $_{HIL}$, nominal full-size battery pack parameters by the subscript $_{BP}$, identified parameters by the subscript $_{ID}$, and scaled-up control-oriented model parameters by the subscript $_{COM}$.

Figure 5: The simulation results for different step sizes

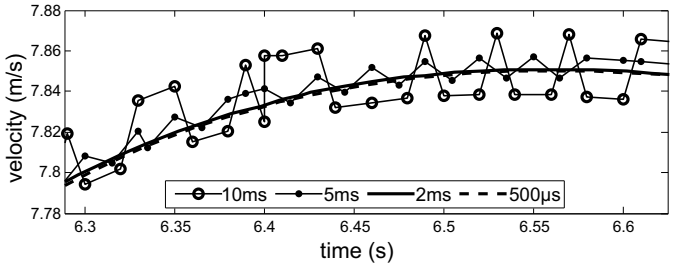

To properly scale the resistance, the new dimensionless parameter in (20) can be used to relate the identified parameters to the scaled-up control-oriented model.

$$\pi_4 = \frac{RQ}{V\tau} \tag{20}$$

Again, as the simulations should have the same time scale, the characteristic times are equal, and the resistor can be scaled according to (21).

$$R_{COM} = \frac{V_{HIL}}{V_{ID}} \frac{Q_{ID}}{Q_{HIL}} R_{ID} = 646.6\ m\Omega \tag{21}$$

6 HIL Simulation Results

In every numerical simulation, the process of convergence study is of great importance. It is essential that the simulation results be free of numerical errors such as integral error and discretization of simulation time. On the other hand, reducing time steps and integration tolerances increases the computational time, and it is possible that the simulation could fall behind real-time requirements.

To solve the high-fidelity model in the HIL setup, the explicit third order Runge-Kutta integrator is used. The result of such an explicit method converges to the correct solution by reducing the time step. When the solution changes negligibly with reducing the time step, it can be inferred that the solution has converged. Figure 5 shows the result of the convergence study conducted for solving the high-fidelity model in LabVIEW. It can be seen that the time step of 2ms gives satisfactory results, hence is used in this simulation.

With the developed setup, a full HIL test can be done on the designed controller. Figure 6 shows the tracking performance of the engine-generator set in the virtual model simulation. As a result of the close tracking of the engine-generator set, the reference battery power (the set-point to the battery cycler) closely follows the optimal trajectory that the optimal controller had calculated for the FTP75 drive cycle. Figure 7 also shows that the battery cycler can very well track the set-points. Therefore, one can conclude that the actual battery in powertrain will behave very similar to the simple control-oriented model.

Figure 8 shows the state of charge trajectory of these cells, and what the controller had predicted based on the control-oriented model, for the first part of

Figure 6: Tracking performance of the lower level controllers of the engine-generator set

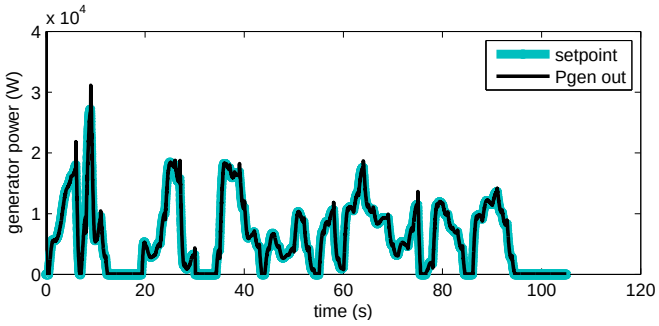

Figure 7: Battery power in the HIL simulation

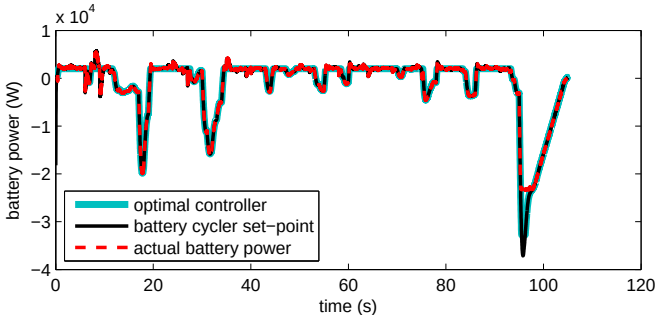

Figure 8: HIL simulation results for the state of charge trajectory for the first part of the FTP75 drive cycle

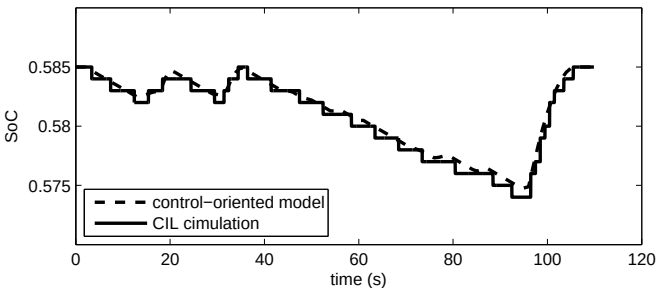

the FTP75 drive cycle. As can be seen, the controller can successfully predict the battery's behavior, using the control-oriented model.

It should be noted that the Li-ion battery parameters, unlike NiMH batteries, change with variations of state of charge. However, in this FTP75 simulation, and in general, in every HEV operation, the variation of state of charge is small; thus the battery parameters remain very close to the identified parameters. This assumption

that was made in the controller design process can now be justified by our HIL simulation results.

As the battery – the most critical component of the powertrain – behaves as predicted by the control-oriented model, one can examine such results and conclude that the optimal controller is indeed able to predict the optimal behavior of the system [8]. Since the lower-level controllers can force the system to follow the optimal controller set-points (see Figures 6 and 7), the behavior of the system with the use of the optimal controller is, therefore, optimal.

7 Conclusions

This article presented the development of a battery HIL setup which can reduce the time and cost of the development of HEV power management controllers. By employing a scaled-down battery cycler in the HIL setup, an accurate control-oriented model was found, which was scaled to arbitrary target battery size without loss in accuracy, using Buckingham's Pi Theorem.

With this control-oriented model, the power management controller was designed. To test the controller, it was programmed into a rapid-prototyping ECU in the HIL setup. A real-time computer was used to solve the virtual high-fidelity models of the components in the powertrain. For the HEV battery, the physical battery in the HIL setup was scaled and driven by the battery cycler in real-time to enhance the accuracy of the simulation.

The HIL results showed that the identified control-oriented model can accurately capture the important dynamics of the system, and as the lower level controllers of different components ensured tracking of the set-points, the outcome of the controller was according to the control-oriented model, and therefore, optimal.

8 Acknowledgments

Financial support for this research has been provided by the Natural Sciences and Engineering Research Council of Canada (NSERC), Toyota, and Maplesoft.

Nomenclature

α	Engine constant
β	Engine constant
η_m	Total driveline efficiency
π_1	Pi group related to battery voltage
π_2	Pi group related to battery capacity
π_3	Pi group related to battery resistance
π_4	Modified Pi group related to battery resistance

τ	Characteristic time
τ_{BP}	Characteristic time in the full-size battery pack
τ_{HIL}	Characteristic time in HIL setup
SoC	Battery state of charge
I	Current
I_{BP}	Full-size battery pack current
I_{HIL}	Battery current in HIL setup
J	Cost function
P	Power
P_b	Battery power
P_e	Electric power demand
P_{BP}	Battery power in full-size battery pack
P_d	Mechanical power demand at wheels
P_{gen}	Generator output power
P_{HIL}	Battery power in HIL setup
Q	Battery capacity
Q_{COM}	Battery pack capacity in control-oriented model
Q_{BP}	Nominal full-size battery pack capacity
Q_{HIL}	Nominal battery capacity in HIL setup
Q_{ID}	Identified battery capacity in HIL setup
R	Battery equivalence series resistance
R_{COM}	Battery pack resistance in the control-oriented model
R_{BP}	Full-size battery pack resistance
R_{HIL}	Battery resistance in HIL setup
R_{ID}	Identified battery resistance in HIL setup
V	Voltage
V_{COM}	Battery pack voltage in control-oriented model
V_{BP}	Nominal full-size battery pack voltage
V_{HIL}	Nominal battery voltage in HIL setup
V_{ID}	Identified battery voltage in HIL setup
V_{oc}	Battery open-circuit voltage

References

[1] J. D. Gonder, "Route-based control of hybrid electric vehicles," in *SAE 2008 World Congress*, 2008.

[2] A. Sciarretta and L. Guzzella, "Control of hybrid electric vehicles," *Control Systems, IEEE*, vol. 27, no. 2, pp. 60–70, apr. 2007.

[3] H. Borhan, C. Zhang, A. Vahidi, A. Phillips, M. Kuang, and S. Di Cairano, "Nonlinear model predictive control for power-split hybrid electric vehicles," in *Decision and Control (CDC), 2010 49th IEEE Conference on*, dec. 2010, pp. 4890–4895.

[4] A. Taghavipour, N. L. Azad, and J. McPhee, "An optimal power management strategy for power split plug-in hybrid electric vehicles," *International Journal of Vehicle Design, in press*, in press.

[5] B. Sampathnarayanan, L. Serrao, S. Onori, G. Rizzoni, and S. Yurkovich, "Model predictive control as an energy management strategy for hybrid electric vehicles," *ASME Conference Proceedings*, vol. 2009, no. 48937, pp. 249–256, 2009.

[6] L. Serrao, S. Onori, and G. Rizzoni, "A comparative analysis of energy management strategies for hybrid electric vehicles," *Journal of Dynamic Systems, Measurement, and Control*, vol. 133, no. 3, 2011.

[7] R. S. Razavian, N. L. Azad, and J. McPhee, "On real-time optimal control of a series hybrid electric vehicle with an ultra-capacitors," in *American Control Conference (ACC), 2012*, jun. 2012, pp. 547–552.

[8] R. S. Razavian, A. Taghavipour, N. L. Azad, and J. McPhee, "Design and evaluation of a real-time fuel-optimal control system for series hybrid electric vehicles," *International Journal of Electric and Hybrid Vehicles*, vol. 4, no. 3, pp. 260–288, 2012.

[9] N. Kim, S. Cha, and H. Peng, "Optimal control of hybrid electric vehicles based on pontryagin's minimum principle," *Control Systems Technology, IEEE Transactions on*, vol. 19, no. 5, pp. 1279–1287, sep. 2011.

[10] N. Kim, S. W. Cha, and H. Peng, "Optimal equivalent fuel consumption for hybrid electric vehicles," *Control Systems Technology, IEEE Transactions on*, vol. 20, no. 3, pp. 817–825, May 2012.

[11] R. Cipollone and A. Sciarretta, "Analysis of the potential performance of a combined hybrid vehicle with optimal supervisory control," in *Computer Aided Control System Design, 2006 IEEE International Conference on Control Applications, 2006 IEEE International Symposium on Intelligent Control, 2006 IEEE*, oct. 2006, pp. 2802–2807.

[12] S. Stockar, V. Marano, G. Rizzoni, and L. Guzzella, "Optimal control for plug-in hybrid electric vehicle applications," in *American Control Conference (ACC), 2010*, june 30-july 2 2010, pp. 5024 –5030.

[13] L. Serrao and G. Rizzoni, "Optimal control of power split for a hybrid electric refuse vehicle," in *American Control Conference (ACC), 2008*, jun. 2008, pp. 4498 –4503.

[14] D. E. Kirk, *Optimal Control Theory: An Introduction.* Dover Publications, Inc., 2004.

[15] D. Ambuhl and L. Guzzella, "Predictive reference signal generator for hybrid electric vehicles," *Vehicular Technology, IEEE Transactions on*, vol. 58, no. 9, pp. 4730–4740, nov. 2009.

[16] L. Brand, "The pi theorem of dimensional analysis," *Archive for Rational Mechanics and Analysis*, vol. 1, pp. 35–45, 1957, 10.1007/BF00297994.

[17] M. D. Petersheim and S. N. Brennan, "Scaling of hybrid-electric vehicle powertrain components for hardware-in-the-loop simulation," *Mechatronics*, vol. 19, no. 7, pp. 1078–1090, 2009, special Issue on Hardware-in-the-loop simulation.

[18] M. Petersheim and S. Brennan, "Scaling of hybrid electric vehicle powertrain components for hardware-in-the-loop simulation," in *Control Applications, 2008. CCA 2008. IEEE International Conference on*, sept. 2008, pp. 720–726.

[19] N. Dalfio, A. Morgando, and A. Sorniotti, "Electro-hydraulic brake systems: design and test through hardware-in-the-loop simulation," *Vehicle System Dynamics*, vol. 44, no. supl, pp. 378–392, 2006.

[20] J.-C. Lee and M.-W. Suh, "Hardware-in-the loop simulator for abs/tcs," in *Control Applications, 1999. Proceedings of the 1999 IEEE International Conference on*, vol. 1, 1999, pp. 652–657.

[21] Y. Xiao-kun, H. Hong-wen, P. Lian-yun, and Z. Xiaolin, "Hardware-in-the-loop simulation on a hybrid power system," in *Power Electronics Systems and Applications (PESA), 2011 4th International Conference on*, jun. 2011, pp. 1–5.

[22] L. Gauchia and J. Sanz, "A per-unit hardware-in-the-loop simulation of a fuel cell/battery hybrid energy system," *Industrial Electronics, IEEE Transactions on*, vol. 57, no. 4, pp. 1186–1194, april 2010.

[23] A. Hentunen, J. Suomela, A. Leivo, M. Liukkonen, and P. Sainio, "Hardware-in-the-loop verification environment for heavy-duty hybrid electric vehicles," in *Vehicle Power and Propulsion Conference (VPPC), 2010 IEEE*, sept. 2010, pp. 1–6.

[24] O. Grondin, L. Thibault, P. Moulin, A. Chasse, and A. Sciarretta, "Energy management strategy for diesel hybrid electric vehicle," in *Vehicle Power and Propulsion Conference (VPPC), 2011 IEEE*, sept. 2011, pp. 1–8.

[25] Y.-H. Hung, C.-H. Wu, S.-M. Lo, B.-R. Chen, E.-I. Wu, and P.-Y. Chen, "Development of a hardware in-the-loop platform for plug-in hybrid electric vehicles," in *Computer Communication Control and Automation (3CA), 2010 International Symposium on*, vol. 1, may 2010, pp. 45–48.

[26] R. A. McGee, "Model based control system design and verification for a hybrid electric vehicle," SAE Technical Paper, Tech. Rep., jun. 2003.

[27] D. Ramaswamy, R. McGee, S. Sivashankar, A. Deshpande, J. Allen, K. Rzemien, and W. Stuart, "A case study in hardware-in-the-loop testing: Development of an ecu for a hybrid electric vehicle," SAE Technical Paper, Tech. Rep., 03 2004.

[28] J.-M. Timmermans, J. Van Mierlo, P. Lataire, F. Van Mulders, and Z. McCaffree, "Test platform for hybrid electric power systems: Development of a hil test platform," in *Power Electronics and Applications, 2007 European Conference on*, sept. 2007, pp. 1–7.

[29] L. Wang, Y. Zhang, C. Yin, H. Zhang, and C. Wang, "Hardware-in-the-loop simulation for the design and verification of the control system of a series parallel hybrid electric city-bus," *Simulation Modelling Practice and Theory*, vol. 25, pp. 148–162, 2012.

[30] Z. Xiaowei, H. Hongwen, and X. Rui, "Hardware in loop simulation for vehicle controller in hev based on dspace," in *Advanced Computer Theory and Engineering (ICACTE), 2010 3rd International Conference on*, vol. 2, aug. 2010, pp. 489–492.

[31] L. F. Xu, J. Q. Li, J. F. Hua, X. J. Li, and M. G. Ouyang, "Hardware in the loop simulation of vehicle controller unit for fuel cell/battery hybrid bus," in *Vehicle Power and Propulsion Conference, 2009. VPPC '09. IEEE*, sept. 2009, pp. 1777–1782.

[32] C. Dufour, T. Ishikawa, S. Abourida, and J. Belanger, "Modern hardware-in-the-loop simulation technology for fuel cell hybrid electric vehicles," in *Vehicle Power and Propulsion Conference (VPPC), 2007*, sept. 2007, pp. 432–439.

[33] S. Shen, J. Zhang, X. Chen, Q.-C. Zhong, and R. Thornton, "Isg hybrid powertrain: a rule-based driver model incorporating look-ahead information," *Vehicle System Dynamics*, vol. 48, no. 3, pp. 301–337, 2010.

[34] H. F. LAM and W. H. Liao, "Semi-active control of automotive suspension systems with magnetorheological dampers," in *Smart structures and integrated systems*, vol. 4327, March 2001, pp. 125–136.

[35] J. Wagner and J. Furry, "A real-time simulation environment for the verification of automotive electronic controller software," *International Journal of Vehicle Design*, vol. 13, no. 4, pp. 365–377, 1992.

[36] W. Lee, M. Yoon, and M. Sunwoo, "A cost- and time-effective hardware-in-the-loop simulation platform for automotive engine control systems," *Proceedings of the Institution of Mechanical Engineers. Part D, Journal of automobile engineering*, vol. 217, pp. 41–52, 2003.

[37] C. Ma, M. Xu, and H. Wang, "Dynamic emulation of road/tyre longitudinal interaction for developing electric vehicle control systems," *Vehicle System Dynamics*, vol. 49, no. 3, pp. 433–447, 2011.

[38] T. S. Dao, A. Seaman, J. McPhee, and K. Shigematsu, "Symbolic modeling of a series-hybrid electric vehicle for real-time simulations," in *JSAE Annual Congress*, May 2011.

[39] M. Saeedi, "A mean value internal combustion engine model in maplesim," Master's thesis, University of Waterloo, Department of Mechanical and Mechatronics Engineering, 2010.

[40] T. S. Dao, C. P. Vyasarayani, and J. McPhee, "Simplification and order reduction of lithium-ion battery model based on porous-electrode theory," *Journal of Power Sources*, vol. 198, no. 0, pp. 329–337, 2012.